

Magnetic properties of a glassy ferromagnet: $\text{Fe}_{78}\text{B}_{13}\text{Si}_9$

Anil K. Bhatnagar and N. Ravi

School of Physics, University of Hyderabad, Hyderabad 500 134, India

(Received 18 August 1982; revised manuscript received 22 November 1982)

METGLAS 2605S2, $\text{Fe}_{78}\text{B}_{13}\text{Si}_9$, has been investigated over a temperature range of 77–900 K by ^{57}Fe Mössbauer spectroscopy. The analysis of the distribution of hyperfine fields indicates two peaks. The maximum of the dominant peak varies with temperature. Another smaller peak is centered around 100 kOe. The $H_{\text{eff}}(T)/H_{\text{eff}}(0)$ vs T/T_c deviates from the Brillouin curve for spin $S=1$ but agrees well with the modified Handrich's expression proposed earlier by Prasad *et al.* The temperature dependence of the average hyperfine field $H_{\text{eff}}(T)$ can be described well by $H_{\text{eff}}(T)=H_{\text{eff}}(0) [1-B_{3/2}(T/T_c)^{3/2}-C_{5/2}(T/T_c)^{5/2}]$ with $H_{\text{eff}}(0)=276$ kOe, $B_{3/2}=0.23$, and $C_{5/2}=0.32$ for $T/T_c < 0.7$ indicative of the existence of spin-wave excitations. The Curie and the crystallization temperatures are found to be 733 ± 1 K and 836 ± 2 K by the zero-velocity counting method with the use of a heating rate of 5 K/min. The quadrupole splitting just above T_c is (0.30 ± 0.04) mm/sec whereas the average quadrupole splitting below T_c is zero. The critical exponent β , in the expression $H_{\text{eff}}(T)/H_{\text{eff}}(0)=D(1-T/T_c)^\beta$ is found to be 0.34 ± 0.02 from the measurements in the temperature region $0.68 < T/T_c < 1$. The isomer shift shows a temperature dependence above 200 K due to a second-order Doppler shift.

I. INTRODUCTION

The magnetic metallic glasses produced by rapid quenching of a melt of iron-based transition-metal–metalloid systems have been of scientific and technological interest in the recent past.¹ Although these glasses lack long-range crystalline order they show ferromagnetic order.² Due to random or disordered atomic arrangement in magnetic-metallic glasses their characteristic magnetic parameters, like exchange interactions, magnetic moments, hyperfine fields, etc., have a distribution of values instead of unique values. Also, since the glassy state represents a metastable state they tend to show structural relaxation with time which gets accelerated at higher temperatures. At high enough temperatures they crystallize irreversibly in a more stable state. Crystallization usually destroys most of their useful magnetic and mechanical properties. Therefore, much experimental effort has been spent to improve the thermal stability of metallic glasses by experimenting with compositional changes in these glasses.

The most studied metallic glass system is $\text{Fe}_x\text{B}_{1-x}$ ($0.72 \leq x \leq 0.86$) which may even be called the basic magnetic-metallic glass system.^{3–8} In a binary system, it is easier to interpret experimental results theoretically. However, it has not satisfied the practical application requirements. Therefore,

there have been consistent efforts by numerous investigators to improve thermal stability and magnetic properties of the Fe-B system by substituting either another transition metal (Ni, Co, etc.) or another metalloid element (P, Si, etc.) or both. It has been found that the inclusion of Si in the Fe-B system improves the thermal stability as well as some magnetic properties.^{5–7} A number of studies have been reported on Fe-B-Si metallic glasses to elucidate their electrical and magnetic properties and thermal stability.^{9–14} Allied Chemical (USA) has recently found that the metallic glass having the nominal composition $\text{Fe}_{78}\text{B}_{13}\text{Si}_9$ (METGLAS 2605S2) has extremely low core loss at distribution and power transformer frequencies and inductions. We, therefore, have taken up detailed studies of commercially available $\text{Fe}_{78}\text{B}_{13}\text{Si}_9$ to elucidate its electrical and magnetic properties and their dependence on aging, temperature, annealing, etc. In this paper we report a detailed study of magnetic properties of $\text{Fe}_{78}\text{B}_{13}\text{Si}_9$ by ^{57}Fe Mössbauer spectroscopy from 77 to 900 K, as well as preliminary work on its crystallization behavior.

II. EXPERIMENTAL

Metallic glass $\text{Fe}_{78}\text{B}_{13}\text{Si}_9$ (METGLAS 2605S2) was received from Allied Chemical (USA). The Mössbauer spectra at different temperatures

(77–900 K) were recorded along with their mirror images, using an Elscint Mössbauer spectrometer in the constant acceleration mode. Experimental details were essentially the same as reported earlier except that a 25-mCi source was used.¹⁵ A linewidth [full width at half maximum (FWHM)] of 0.28 mm/sec was obtained for natural iron foil in our spectrometer.

III. RESULTS AND DISCUSSIONS

A. Mössbauer spectra and magnetic interactions

Figure 1 displays some of the recorded Mössbauer spectra of an as-received sample of $\text{Fe}_{78}\text{B}_{13}\text{Si}_9$ at temperatures between 77 and 735 K. Spectra at temperatures below 650 K consist of six strongly overlapping broad lines (width 0.6–1.2 mm/sec) and are characteristic of a typical iron-rich metallic glass. However, spectra are still well resolved below 650 K, and therefore hyperfine fields $H_{\text{eff}}(T)$ were determined from the splitting between the first and sixth lines. The data have also been computer fitted using Lorentzian line shapes with variable linewidths, line intensities, and line positions. This gives essentially the same $H_{\text{eff}}(T)$ as directly mea-

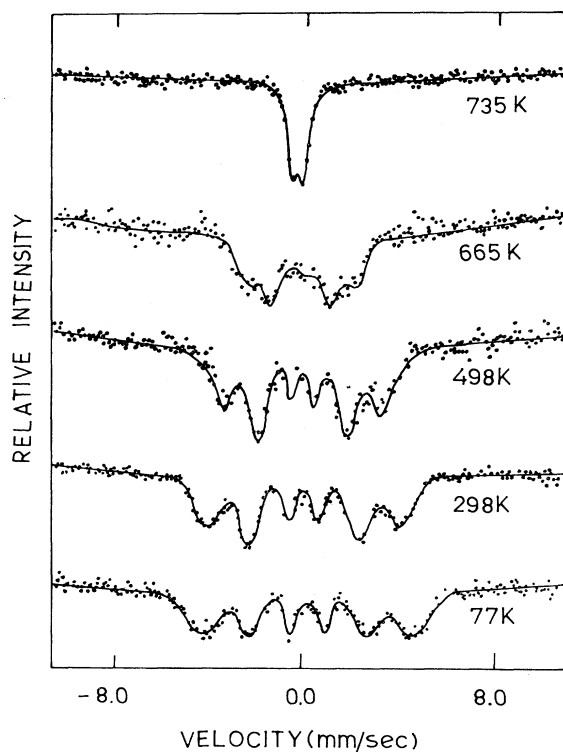


FIG. 1. Transmission Mössbauer spectra of $\text{Fe}_{78}\text{B}_{13}\text{Si}_9$ at various temperatures below the crystallization temperature.

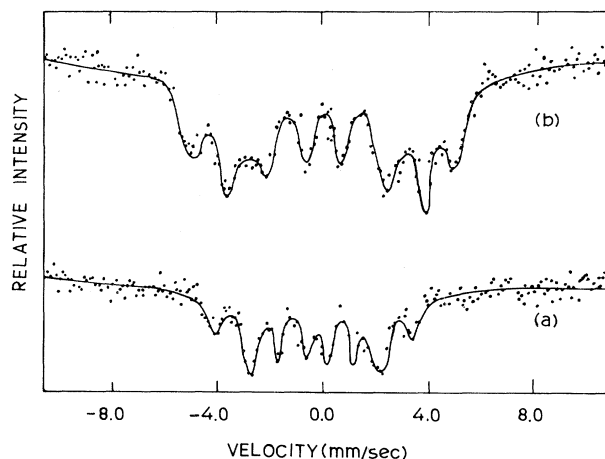


FIG. 2. Mössbauer spectra of the crystallized $\text{Fe}_{78}\text{B}_{13}\text{Si}_9$. (a) at 850 K and (b) at 300 K after cooling from 850 K.

sured. These are listed in Table I. The spectra at and above 665 K become harder to resolve but the ferromagnetic state remains up to 715 K. At and above 735 K a paramagnetic spectrum is obtained until 850 K, the temperature at which a complex spectrum is observed due to crystallization of the sample as shown in Fig. 2.

Mössbauer spectra between 296 and 650 K show slight asymmetry in linewidths and intensities for lines 1 and 6, and lines 2 and 5. Intensities of lines 2 and 5 are larger than that of lines 1 and 6. The magnetization direction of a sample can be determined by knowing the relative intensities of the second (fifth) to the first (sixth) lines which theoretically should be $A_{2,5}/A_{1,6} = 4 \sin^2\theta / 3(1 + \cos^2\theta)$, where θ is the angle between the 14.4-keV gamma

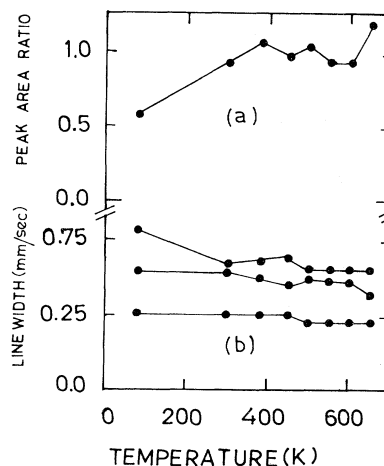


FIG. 3. Linewidths and area ratios of the spectral lines of $\text{Fe}_{78}\text{B}_{13}\text{Si}_9$ as a function of temperature. Here the area ratio is defined as $(A_2 + A_5)/(A_1 + A_6)$.

rays of ^{57}Fe and the direction of the magnetic hyperfine field.¹⁶ The ratio $A_{2,5}/A_{1,6}$ can vary from 0 to $\frac{4}{3}$ as θ changes from 0° to 90° . For a completely randomly distributed magnetic moment directions this ratio is $\frac{2}{3}$. Since the lines are broad in glassy alloys the ratios under the lines are usually compared rather than the intensity ratios. It was found that a good fit does not necessarily give the same area for lines 1 and 6, lines 2 and 5, and lines 3 and 4. Because of this reason, ratio $(A_2 + A_5)/(A_1 + A_6)$ vs T has been plotted in Fig. 3(a) in which two successive points are connected by a straight line. It is observed from Fig. 3(a) that the magnetization axis does not lie in the plane of the ribbon at 77 K and is close to being perpendicular to the ribbon axis. However, as temperature is increased the magnetization axis tilts towards the ribbon plane and at high temperatures it becomes parallel to the plane of the ribbon. It has been established earlier that clamping of the sample introduces stress in the sample which will change the direction of the magnetization axis.¹⁶ Since our samples were mounted on an annular ring we suspect that this behavior may be due to stress in the sample.

Figure 3 also shows average linewidths of lines 1 and 6, 2 and 5, and 3 and 4. It is observed that the linewidths decrease with increasing temperature. Partially this may be due to the finite thickness of the absorber but it also indicates that the distribution of hyperfine fields is becoming narrower. This is confirmed by the observed decrease in FWHM of hyperfine field distribution, $P(H)$ vs H curves with increase in temperatures as discussed in Sec. III B.

B. Hyperfine field distribution

Mössbauer spectra of glassy ferromagnets have been observed to consist of six broad lines as shown in Fig. 1 and discussed in the preceding section. This broadening of Mössbauer lines has always been attributed to the random environment surrounding the Mössbauer nuclei which gives rise to a large number of structurally inequivalent sites.³ This disordered arrangement gives rise to a distribution of exchange interaction. We have determined the hyperfine field distribution $P(H)$ for these spectra using the Fourier series method developed by Window.¹⁷ The intensity ratio of the sextet is assumed to be $3:b:1:1:b:3$, and by changing the value of b a smooth and better fit can be obtained. (In the present case $b=2.3$ gave the best fit at all temperatures.) The $P(H)$ distribution curves at temperatures 296, 380, 600, and 650 K are shown in Fig. 4. Solid curves in Fig. 5 at 296 and 600 K are the best-fit results obtained by the inclusion of $P(H)$ in the computer fit of data. Oscillatory features, which

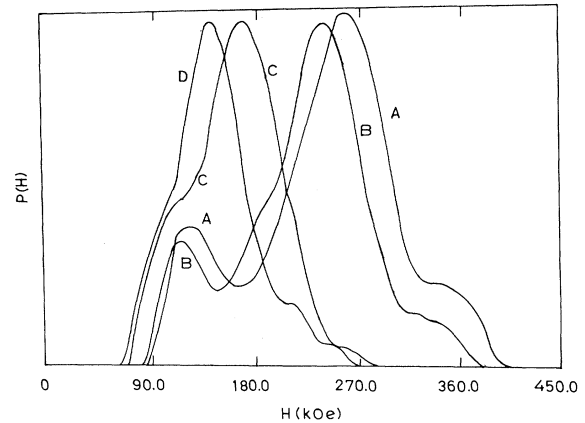


FIG. 4. Hyperfine field distribution $P(H)$ of $\text{Fe}_{78}\text{B}_{13}\text{Si}_9$ at A, 296 K; B, 380 K; C, 600 K; D, 650 K.

are always found in $P(H)$ due to the truncated Fourier series, are not shown because these do not possess any significance. The $P(H)$ curves of $\text{Fe}_{78}\text{B}_{13}\text{Si}_9$, as shown in Fig. 4, have one dominant peak centered around a value of magnetic field called the most probable field H_{p1} and another small peak H_{p2} at a lower field of ~ 100 kOe. Thus there is a broad range of H values centered around a high field value (the most probable field H_{p1}) and a small range of H values centered around $H_{p2} \sim 100$ kOe. As seen from Fig. 4, the dominant peak shifts towards the lower field values as the temperature is increased which of course is expected. However, the smaller peak does not shift so much and at high enough temperatures it starts overlapping with the dominant peak. The shape of the dominant peak is found to be nearly independent of temperature indi-

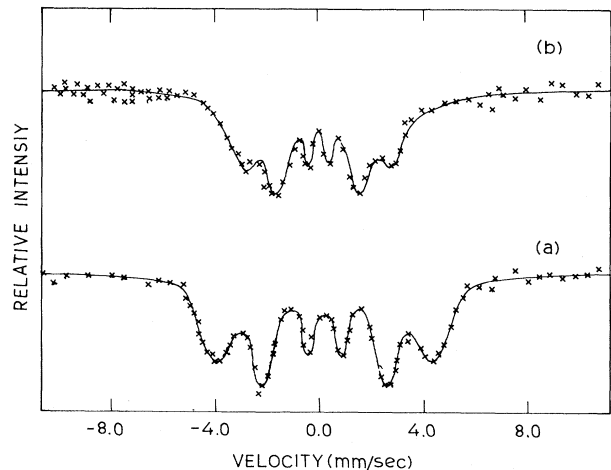


FIG. 5. Mössbauer spectra of $\text{Fe}_{78}\text{B}_{13}\text{Si}_9$. Fit using the deduced hyperfine field distribution $P(H)$ (a) at 296 K, and (b) at 600 K. Crosses represent the experimental points.

TABLE I. Results of the hyperfine field distribution analysis.

Temp. (K)	$H_{\text{eff}}(T)$ (kOe)	$H_{p1}(T)$ (kOe)	$H_m(T)$ (kOe)	$(\Delta H)_1$ (kOe)	$H_{p2}(T)$ (kOe)	$(\Delta H)_2$ (kOe)
77	273.17	279.38	271.77	99.0	130.50	45.0
296	251.88	270.00	251.09	81.0	126.00	36.0
380	234.36	250.24	234.62	76.5	119.25	22.5
450	221.00	229.24	229.73	76.5	114.75	22.5
500	207.11	207.00	216.88	72.0	112.50	22.5
550	181.34	189.00	208.71	67.5	105.75	22.5
600	172.32	175.50	195.92	54.0		
650	145.94	150.75	186.74	40.5		

cating that all the components of $P(H)$ must have nearly the same temperature dependence. Table I lists the values of $H_{\text{eff}}(T)$ obtained from the fit of spectra to the Lorentzian sextet, $H_{p1}(T)$ the most probable field value of the dominant peak and the mean field value $H_m(T)$ defined as

$$H_m = \int HP(H)dH / \int P(H)dH .$$

$H_{\text{eff}}(T)$ is observed to be smaller than H_{p1} by a few percent. Table I also lists values of $H_{p2}(T)$ and FWHM $(\Delta H)_1$ and $(\Delta H)_2$ for the dominant peak and the smaller peak as well. Figure 6 shows the temperature dependence behavior of (H_{p1}) and $(\Delta H)_1$ for the dominant peak and (H_{p2}) and $(\Delta H)_2$ for the smaller peak in the $P(H)$ curves. At high temperatures since two peaks start overlapping it was not possible to determine $(\Delta H)_2$. Since $(\Delta H)_1$ decreases with temperature, it indicates that various H values contained in the dominant peak have nearly the same temperature dependence as that of $(\Delta H)_1$. The width of smaller peak is almost temperature independent although it is a little lower at higher temperatures.

It is also worthwhile to compare our results with some previous works on $P(H)$ evaluation in ferromagnetic glasses. It has generally been found that there is one dominant peak in the $P(H)$ curve.^{3,18-20} Two peaks have been observed in $\text{Fe}_{32}\text{Ni}_{36}\text{Cr}_{14}\text{P}_{12}\text{B}_6$ (METGLAS 2826A) by Chien.²¹ The second smaller peak in the $P(H)$ curve of this sample at low fields has been interpreted by Chien arising from the presence of some Cr atoms as near neighbors of the Fe atoms. It was also argued that since Cr is antiferromagnetic, it is expected that although the average exchange interaction between Fe and Fe, and Fe and Ni atoms is ferromagnetic and of comparable magnitude, the average exchange interaction between Fe and Cr atoms may be antiferromagnetic. This may lead to two peaks in $P(H)$ as observed. However, in $\text{Fe}_{78}\text{B}_{13}\text{Si}_9$ sample the only ferromagnetic species are Fe atoms; therefore, the origin of

the second peak must lie in some other interaction. It is possible that the second peak arises from a particular near-neighbor interaction, which requires further investigation.

At this point a comparison between the behavior of disordered alloys and metallic glasses merits attention. It has been reported that in disordered alloys such as FeNi_3 , etc., the most probable H_p field and the observed hyperfine field, $H_{\text{eff}}(T)$, at a given temperature T are almost in exact agreement with each other.²² On the other hand, in the case of quenched Fe-Mn alloys this difference between H_p and $H_{\text{eff}}(T)$ is considerably larger at low temperatures and this difference narrows down with the increase in temperature.²³ Our observation of slight difference between the observed average hyperfine field and the most probable field is in accordance with the previously reported trend.^{3,23} This difference narrows down with increasing temperature and agrees reasonably well with the experimental values

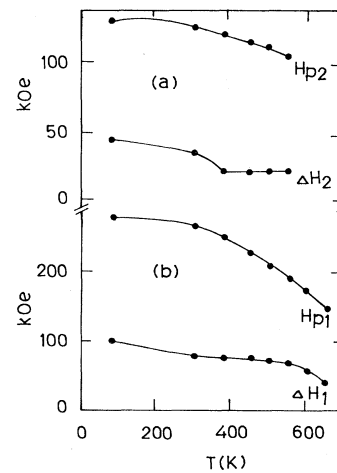


FIG. 6. Temperature dependence of the field H_p of the peak in $P(H)$ and full width at half maximum of $\text{Fe}_{78}\text{B}_{13}\text{Si}_9$ (a) small peak, (b) dominant peak.

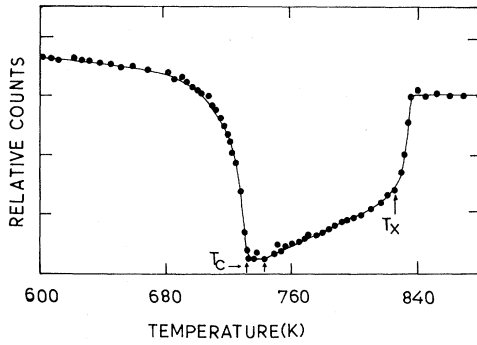


FIG. 7. Count rate at zero Doppler velocity as a function of temperature.

at high temperatures. This is also in conformity with the intensity decrease and the disappearance of the less intense second peak in the $P(H)$ curve with the increase of temperature.

C. Curie and crystallization temperatures

An accurate determination of the Curie temperature was done by performing a zero-velocity counting method.³ The integrated counts were accumulated for a fixed time of 50 sec while the temperature was raised at the rate of 5 K/min from 300 to 900 K. The results are displayed in Fig. 7 in the temperature interval of 600–900 K.

The Curie temperature is defined to be that temperature at which the count rate decreases rapidly due to the disappearance of the magnetic ordering. From Fig. 7 the Curie temperature is found to be 733 ± 1 K. Figure 7 also shows that the count rate starts increasing at 744 K first at a slow rate and then sharply at 826 K, and finally the count rate becomes constant at 836 K. The increase in the count rate at 744 K is due to the second-order Doppler ef-

fect and also may be due to the partial crystallization resulting in the precipitation of iron compounds which have higher Curie temperatures. At $T = 836 \pm 2$ K the amorphous phase gets fully crystallized. This has been confirmed by the complex Mössbauer spectra obtained at 850 K as shown in Fig. 2. Curie temperatures of some other Fe-B-Si metallic glasses are compared with the $\text{Fe}_{78}\text{B}_{13}\text{Si}_9$ sample in Table II.

D. Temperature dependence of $H_{\text{eff}}(T)$

The temperature dependence of the reduced average magnetic hyperfine fields [$H_{\text{eff}}(T)/H_{\text{eff}}(0)$] vs (T/T_c) is plotted in Fig. 8 along with the Brillouin curve for $S=1$. Experimental data lie below the Brillouin curve as observed for other metallic glasses. This observation is usually attributed to the distribution of exchange interactions in glassy ferromagnets arising from the random environment around magnetic atoms. Among other theoretical calculations^{2,24–26} which explain this behavior, Handrich²⁴ obtained the following closed analytical expression for the reduced magnetization of an amorphous ferromagnet:

$$m(T) = \frac{M(T)}{M(0)} = \frac{1}{2} B_s[(1+\delta)x] + \frac{1}{2} B_s[(1-\delta)x], \quad (1)$$

where B_s is the Brillouin function for spin S , $x = (3S/S+1)(m/t)$, and $t = T/T_c$. The parameter δ is a measure of random fluctuations in the exchange interaction and its value lies between 0 and 1. Equation (1) reduces, when $\delta=0$, to the formula for the reduced magnetization applicable to crystalline ferromagnets. Equation (1) does predict the $m(t)$ vs t curve flatter and lower than the Brillouin

TABLE II. Coefficients B , $B_{3/2}$, C , $C_{5/2}$, quadrupole split (QS), and Curie temperature T_c of some metallic glasses.

System	$B_{3/2}$	$C_{5/2}$	B ($10^{-6} \text{ K}^{-3/2}$)	C ($10^{-8} \text{ K}^{-5/2}$)	QS (mm/sec)	T_c	Ref.
$\text{Fe}_{80}\text{B}_{20}$	0.40	0.17	22	1.2		685	33
$\text{Fe}_{40}\text{Ni}_{40}\text{P}_{14}\text{B}_6$	0.47	0.08	38	1.2	0.46	537	33,16
$\text{Fe}_{40}\text{Ni}_{40}\text{B}_{20}$	0.40	0.06	22	0.43		695	28
$\text{Fe}_{82}\text{B}_{12}\text{Si}_6$	0.34	0.21			0.45	658	10
$\text{Fe}_{74}\text{Co}_{10}\text{B}_{16}$	0.466					760	37
$\text{Fe}_{81}\text{B}_{13.5}\text{Si}_{3.5}\text{C}_2$	0.47				0.37	698	38
$\text{Fe}_{75.4}\text{B}_{14.2}\text{Si}_{10.4}$	0.30	0.16			0.46	701	13
$\text{Fe}_{40}\text{Ni}_{38}\text{Mo}_4\text{B}_{18}$	0.34	0.16	23	1.7		608	39
$\text{Fe}_{78}\text{B}_{13}\text{Si}_9$	0.23	0.32	10.4	2.4	0.30	733	Present work
Crystalline Fe	0.114	0.04	3.4	0.1		1042	35
Crystalline Ni	0.117	0.15	7.5	1.5		627	35

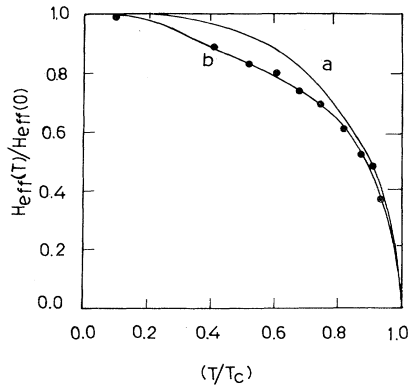


FIG. 8. Reduced hyperfine magnetic field vs reduced temperature of $\text{Fe}_{78}\text{B}_{13}\text{Si}_9$. Solid spheres represent the experimental points. The solid curves *a* and *b* are the results obtained from Eq. (1) for $\delta=0$ and $\delta=0.6(1-t^2)$, respectively.

curve. Since experimentally it has been found that $H_{\text{eff}}(T) \propto M(T)$, experimental data is compared with Eq. (1) using δ as a fitting parameter.

Previously, values of δ as high as 0.5 have been used to show a qualitative agreement between experiments and Handrich's model but quantitative agreement remained unsatisfactory.^{3,16,18,27} In an earlier paper from this laboratory, it has been shown that the quantitative agreement between experimental points and Eq. (1) can be improved greatly if δ is assumed to be temperature dependent.¹⁵ In particular, when $\delta = \delta_0(1-t^2)$ was substituted in Eq. (1), it gave a good fit to the experimental points for the metallic glasses $\text{Fe}_{74}\text{Co}_{10}\text{B}_{16}$ and $\text{Fe}_{80}\text{B}_{20}$ for $\delta_0 = 0.7$ and 0.65, respectively, and $S = \frac{1}{2}$. Recently, a similar good fit has been obtained for $\text{Fe}_{40}\text{Ni}_{40}\text{B}_{20}$ (VITROVAC 0040) when $\delta = \delta_0(1-t^2)$ with $\delta_0 = 0.6$ and $S = 1$ were assumed.²⁸ We have done a similar fitting for $\text{Fe}_{78}\text{B}_{13}\text{Si}_9$ and find that a good agreement is obtained if $\delta = 0.6(1-t^2)$ is substituted in Eq. (1) as shown in Fig. 8. This indicates that this may generally be true for other ferromagnetic metallic glasses. We are unable to explain this temperature dependence of δ at present, but the good fit which it gives with experimental points when used in Eq. (1) cannot be ignored. It may also be noted that the observed fast decrease of $H_{\text{eff}}(T)/H_{\text{eff}}(0)$ vs t is not only limited to glassy ferromagnets but it is also true for crystalline alloys like Fe_3Al , Fe_3Si , etc.²⁹⁻³¹

It has been suggested that a distribution of exchange interactions would lead to different temperature dependencies of "local" magnetizations which would show up in Mössbauer spectra as different temperature dependence of $H_{\text{eff}}(T)/H_{\text{eff}}(0)$. This means that a large variation in exchange interactions, i.e., large δ , should cause a large broadening

for $t \geq 0.8$, if δ remained constant throughout the temperature interval of 0 to T_c , as some of local magnetization region would vanish due to their lower T_c .³² No such broadening of Mössbauer lines has been observed in this work and, in fact, these are found to become narrower with increase in temperature. However, if one assumes $\delta = \delta_0(1-t^2)$ then δ decreases with t , one should expect Mössbauer lines to become narrower as observed here. We believe this temperature dependence of δ comes from an interplay of structural fluctuations and spin disorder. At low temperatures spins are sort of frozen but structural disorder is present, hence it is the structural disorder which plays the important role at low temperatures. At $T \simeq T_c$, the spin disorder is so high that the structural disorder does not have much of an influence on the magnetic properties.

E. Spin-wave excitations

It is now well established³³ that $H_{\text{eff}}(T)/H_{\text{eff}}(0)$ for glassy ferromagnets also varies as

$$\frac{H_{\text{eff}}(T)}{H_{\text{eff}}(0)} = 1 - BT^{3/2} - CT^{5/2} - \dots \quad (2)$$

at low temperatures ($T \ll T_c$). This is essentially Bloch's law applied to crystalline ferromagnets. Equation (2) can be written as

$$\frac{\Delta H_{\text{eff}}(T)}{H_{\text{eff}}(0)} = B_{3/2}(T/T_c)^{3/2} + C_{5/2}(T/T_c)^{5/2} + \dots, \quad (3)$$

where $\Delta H_{\text{eff}}(T) = H_{\text{eff}}(0) - H_{\text{eff}}(T)$. The $T^{3/2}$ temperature dependence comes from the excitation of long-wavelength spin waves. This is not surprising as it has been shown by Herring and Kittel³⁴ that spin waves can exist in a continuous ferromagnetic medium as the detailed noncrystalline arrangement of atoms would not be important for long-wavelength excitations. $\Delta H_{\text{eff}}(T)/H_{\text{eff}}(0)$ has been plotted in Fig. 9 as a function of $(T/T_c)^{3/2}$. It is seen that the data points do not lie on a straight line over a large temperature interval but show slight convex curvature. The same trend has also been observed for $\text{Fe}_{82}\text{B}_{12}\text{Si}_6$.¹⁰ A least-squares fit of Eqs. (2) and (3) to the magnetic hyperfine field data gave $B = 10.4 \times 10^{-6} \text{ K}^{-3/2}$, $C = 2.4 \times 10^{-8} \text{ K}^{-5/2}$, $B_{3/2} = 0.23$, and $C_{5/2} = 0.32$ when data $T/T_c \leq 0.7$ are used. In Table II these values are compared with the values of some other ferromagnetic metallic glasses and crystalline ferromagnets. $B_{3/2}$ and $C_{5/2}$ values for $\text{Fe}_{78}\text{B}_{13}\text{Si}_9$ are of smaller magnitude than those observed for other glassy ferromagnets but are still higher than the values obtained for crystalline ferromagnets such as Fe and Ni (0.114 and 0.117,

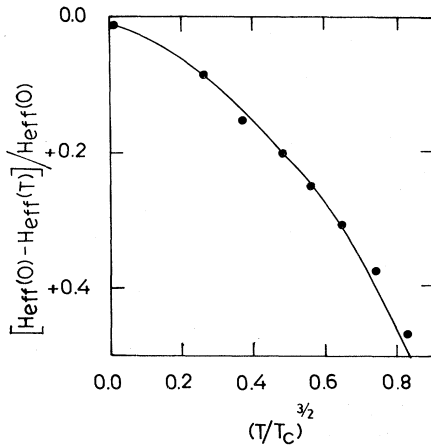


FIG. 9. Fractional change of the hyperfine magnetic field ΔH_{eff} as a function of $(T/T_c)^{3/2}$.

respectively).³⁵ It has been shown by Simpson³⁶ using a phenomenological argument that the structural-disorder-induced variation in the exchange interaction leads to a larger B value. The observation that B is higher for glassy ferromagnets would mean that the spin-wave density of states must be higher for amorphous ferromagnets. Many theoretical calculations do show that the increased disorder in the crystalline structure results in a higher spin-wave density of states for low-frequency excitations. Thus high B values seem to be a characteristic of only the glassy state.

A further analysis of the data can yield the value of the critical exponent β for this glassy ferromagnet. At temperatures close to T_c it is expected that $H_{\text{eff}}(T)/H_{\text{eff}}(0)$ will follow a power law, $H_{\text{eff}}(T)/H_{\text{eff}}(0) = D(1 - T/T_c)^\beta$, where β is one of the critical exponents and D is a constant. A fit of $H_{\text{eff}}(T)/H_{\text{eff}}(0)$ vs $(1 - T/T_c)$ indicates that $\text{Fe}_{78}\text{B}_{13}\text{Si}_9$ does follow this power law in the temperature region $0.68 < T/T_c < 1$, and the fit yields

$$\beta = 0.34 \pm 0.02, \quad D = 1.13 \pm 0.02.$$

The value of β obtained for $\text{Fe}_{78}\text{B}_{13}\text{Si}_9$ is in reasonable agreement with the β values obtained for many other glassy ferromagnets.^{16,28}

F. Quadrupole interaction and isomer shift

Due to the disordered structure in a glassy magnetic solid the Fe site symmetry is not expected to be cubic. Therefore, one would expect the presence of a quadrupole interaction, in addition to the magnetic hyperfine interaction, due to a nonzero electric field gradient (EFG) in all glassy solids. However, this has not been observed in ferromagnetic metallic

glasses for $T < T_c$. It is only above T_c one is able to see the quadrupole split lines in the paramagnetic spectrum.¹⁶ Same results have also been observed in $\text{Fe}_{78}\text{B}_{13}\text{Si}_9$. The principal axis of the EFG tensor varies spatially throughout the glassy sample and hence with respect to the hyperfine magnetic field. Therefore, on the average this interaction becomes zero for a macroscopic glassy sample. Hence, the quadrupole split in the glassy magnetic solids can be measured only for $T > T_c$, the temperature at which the magnetic interaction becomes zero.¹⁶ Our results are in agreement with other magnetic metallic glasses and the observed quadrupole split for $\text{Fe}_{78}\text{B}_{13}\text{Si}_9$ (0.30 ± 0.04 mm/sec) above T_c is little smaller than those for $\text{Fe}_{82}\text{B}_{12}\text{Si}_6$ and $\text{Fe}_{75.4}\text{B}_{14.2}\text{Si}_{10.4}$ listed in Table II.^{10,13} The quadrupole doublet shows a slight asymmetry which has also been observed for other metallic glasses.

Figure 10 shows the temperature dependence of the isomer shift (IS) as determined from the data. A linear variation of IS with temperature is observed above 200 K. This variation is due to the second-order Doppler shift. Theoretically, temperature dependence of IS is found to be linear with temperature at high temperatures if the forces coupling the atoms are assumed to be harmonic. The slope is given by

$$\frac{d\delta(T)}{dT} = -\frac{3kE_\gamma}{2Mc^2}, \quad (4)$$

where c is the velocity of light, M is the atomic mass of the Mössbauer nucleus, k is the Boltzmann constant, and E_γ is the γ -ray energy which in this case is 14.4 keV. The slope given by the above equation comes out to be -7.31×10^{-4} mm/sec K for ^{57}Fe atoms. The slope of $\delta(T)$ vs T in Fig. 10 is -7.1×10^{-4} mm/sec K and is in good agreement with the predicted value. This suggests that the assumptions under which Eq. (4) is derived are valid, i.e., the forces coupling the atoms in amorphous $\text{Fe}_{78}\text{B}_{13}\text{Si}_9$ are harmonic to a good approximation.

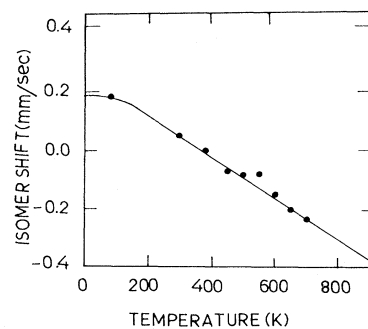


FIG. 10. Temperature dependence of the isomer shift.

IV. CONCLUSIONS

The ferromagnetic metallic glass $\text{Fe}_{78}\text{B}_{13}\text{Si}_9$ has been studied by Mössbauer spectroscopy from 77 to 900 K and the following results have been obtained.

The Mössbauer spectra of $\text{Fe}_{78}\text{B}_{13}\text{Si}_9$ consist of six broad lines indicative of a distribution of hyperfine fields at the Mössbauer nuclei instead of a unique hyperfine field. The analysis of distribution of hyperfine fields shows two peaks, one dominant peak and another small peak. The dominant peak nearly corresponds to the observed average hyperfine field and the small peak is observed near 100 kOe and is probably due to a particular near-neighbor interaction. The Curie and the crystallization temperatures are found to be 733 ± 1 K and 836 ± 2 K, respectively, by the zero-velocity counting method. The temperature dependence of the hyperfine field shows a deviation from the Brillouin curve for $S=1$ but Handrich's expression as modified by Prasad *et al.*¹⁵ satisfactorily explains the observed behavior. Over a range of temperatures the hyperfine magnetic field $H_{\text{eff}}(T)$ follows the Bloch relation

$$H_{\text{eff}}(T) = H_{\text{eff}}(0)(1 - BT^{3/2} - CT^{5/2})$$

with $H_{\text{eff}}(0) = 276$ kOe, $B = 10.4 \times 10^{-6} \text{ K}^{-3/2}$, and $C = 2.4 \times 10^{-8} \text{ K}^{-5/2}$ suggesting the preferential excitation of long-wavelength spin waves. The coefficient of the $T^{3/2}$ term is found to be smaller than the values reported for other metallic glasses but larger than for crystalline ferromagnets. Below the Curie temperature the random orientation of the principal axis of the electric field gradient tensor with respect to the hyperfine magnetic field results in a vanishing average quadrupole split whereas quadrupole splitting above T_c is measured to be 0.30 mm/sec. The temperature dependence of the isomer shift is linear above 200 K and has a slope $-7.1 \times 10^{-4} \text{ mm/sec K}$ and is consistent with the harmonic nature of the atomic binding forces.

ACKNOWLEDGMENTS

The authors would like to thank Dr. R. Jagannathan and Mr. B. Bhanu Prasad for many helpful discussions. The authors are grateful to Mr. A. Datar, Allied Chemical (USA), for sending METGLAS 2605S2 samples. This work has been supported by the Department of Atomic Energy (India) through Research Grant No. 37/7/81-G and DST (India) Grant No. 21(11)/STP-0.

- ¹See, for example, *Rapidly Quenched Metals III*, edited by B. Cantor (The Metals Society, London, 1978), Vols. 1 and 2; *Proceedings of the Conference on Metallic Glasses: Science and Technology*, edited by C. Hargitai, I. Bakonyi, and T. Kemeny (Kultura, Budapest, 1981); *Proceedings of Rapidly Quenched Metals IV* (The Japan Institute of Metals, Sendai, 1982).
- ²A. I. Gubnov, *Fiz. Tverd. Tela* (Leningrad) **2**, 502 (1960).
- ³C. L. Chien, *Phys. Rev. B* **18**, 1003 (1978).
- ⁴C. L. Chien, D. Musser, E. M. Gyorgy, R. C. Sherwood, H. S. Chen, F. E. Luborsky, and J. L. Walter, *Phys. Rev. B* **20**, 283 (1979).
- ⁵T. Kemeny, I. Vincze, B. Fogarassy, and S. Araj, *Phys. Rev. B* **20**, 476 (1979).
- ⁶A. S. Schaafsma, H. Snijders, F. van der Woude, J. Drijver, and S. Radelaar, *Phys. Rev. B* **20**, 4423 (1979).
- ⁷M. W. Ruckman, R. A. Levy, A. Kessler, and R. Hasegawa, *J. Non-Cryst. Solids* **40**, 393 (1980).
- ⁸N. Banerjee, R. Roy, A. K. Majumdar, and R. Hasegawa, *Phys. Rev. B* **24**, 6801 (1981).
- ⁹T. Kemeny, I. Vincze, H. A. Davies, I. W. Donald, and A. Lovas, Central Research Institute for Physics, Budapest, Hungary, Report No. KFKI-1980-103 (unpublished).
- ¹⁰H. N. Ok and A. H. Morrish, *Phys. Rev. B* **22**, 4215 (1980).

- ¹¹J. M. Dubois, M. Bastick, G. La Caer, and C. Tete, *Rev. Phys. Appl.* **15**, 1103 (1980).
- ¹²H. N. Ok and A. H. Morrish, *J. Phys. F* **11**, 495 (1981).
- ¹³H. N. Ok, K. S. Baek, and C. S. Kim, *Phys. Rev. B* **24**, 6600 (1981).
- ¹⁴I. W. Donald, T. Kemeny, and H. A. Davies, *J. Phys. F* **11**, 131 (1981).
- ¹⁵B. Bhanu Prasad, A. K. Bhatnagar, and R. Jagannathan, *Solid State Commun.* **36**, 661 (1980).
- ¹⁶C. L. Chien and R. Hasegawa, *Phys. Rev. B* **16**, 3024 (1977).
- ¹⁷B. Window, *J. Phys. E* **4**, 401 (1971), and references therein.
- ¹⁸T. E. Sharon and C. C. Tsuei, *Phys. Rev. B* **5**, 1047 (1972).
- ¹⁹J. Logan and E. Sun, *J. Non-Cryst. Solids* **20**, 285 (1976).
- ²⁰I. Vincze and E. Babic, *Solid State Commun.* **27**, 1425 (1978).
- ²¹C. L. Chien, *Phys. Rev. B* **19**, 81 (1979).
- ²²A. Narayanasamy, T. Nagarajan, P. Muthukumarasamy, and T. S. Radhakrishnan, *J. Phys. F* **9**, 2261 (1979).
- ²³H. Heller, K. V. Rao, P. G. Dubrunner, and H. S. Chen, *J. Appl. Phys.* **52**, 1753 (1981).
- ²⁴K. Handrich, *Phys. Status Solidi* **32**, K55 (1969).
- ²⁵S. Kobe, *Phys. Status Solidi* **41**, K13 (1970).

- ²⁶S. Kobe and K. Handrich, *Fiz. Tverd. Tela* (Leningrad) **13**, 887 (1971) [*Sov. Phys.—Solid State* **13**, 734 (1971)].
- ²⁷P. J. Schurer and A. H. Morrish, *Solid State Commun.* **30**, 21 (1979).
- ²⁸A. K. Bhatnagar, B. Bhanu Prasad, N. Ravi, R. Jagannathan, and T. R. Anantharaman, *Solid State Commun.* **44**, 905 (1982).
- ²⁹A. Andreeft, H. J. Hunger, and S. Unterricker, *Phys. Status Solidi B* **66**, K23 (1974).
- ³⁰C. Blaauw, H. Hanson, F. van der Woude, and G. A. Sawatzky, *Proceedings of the V International Conference on Mössbauer Spectroscopy* (Czechoslovakian Atomic Energy Commission, Prague, 1975), pp. 10–14.
- ³¹T. J. Burch, K. Raj, P. Jena, J. I. Budnik, V. Niculescu, and W. B. Muir, *Phys. Rev. B* **19**, 2933 (1979).
- ³²Dr. P. J. Schurer (private communication).
- ³³C. L. Chien and R. Hasegawa, *Phys. Rev. B* **16**, 2115 (1977).
- ³⁴C. Herring and C. Kittel, *Phys. Rev.* **81**, 869 (1951).
- ³⁵B. E. Argyle, S. H. Charap, and E. W. Pugh, *Phys. Rev.* **132**, 2051 (1963).
- ³⁶A. W. Simpson, *Wiss. Z. Tech. Hochsch. Dresden* **3**, 1020 (1974).
- ³⁷B. Bhanu Prasad, A. K. Bhatnagar, and R. Jagannathan, in *Proceedings of International Conference on Applications of The Mössbauer Spectroscopy, Jaipur, India, 1981* (INSA, New Delhi, 1981), p. 366.
- ³⁸B. Bhanu Prasad and A. K. Bhatnagar (private communication).
- ³⁹Rajaram and G. Chandra, in *Proceedings of International Conference on Applications of the Mössbauer Spectroscopy, Jaipur, India, 1981*, Ref. 37, p. 357.